

Article

Not peer-reviewed version

# A New Frontier in Hypertension Management: Formulating and Characterizing Subcutaneous Implants using Hot Melt Extrusion

[Kshitij Chitnis](#) , [Nagarjuna Narala](#) , Sagar Narala , [Siva Ram Munnangi](#) , [Sateesh Kumar Vemula](#) , [Michael A Repka](#) \*

Posted Date: 27 December 2023

doi: 10.20944/preprints202312.2064.v1

Keywords: Hypertension, Subcutaneous Implants, Hot Melt Extrusion, Controlled Drug Delivery, Biodegradable, Implantable Drug Delivery



Preprints.org is a free multidiscipline platform providing preprint service that is dedicated to making early versions of research outputs permanently available and citable. Preprints posted at Preprints.org appear in Web of Science, Crossref, Google Scholar, Scilit, Europe PMC.

Copyright: This is an open access article distributed under the Creative Commons Attribution License which permits unrestricted use, distribution, and reproduction in any medium, provided the original work is properly cited.

*Article*

# A New Frontier in Hypertension Management: Formulating and Characterizing Subcutaneous Implants Using Hot Melt Extrusion

Kshitij Chitnis <sup>1</sup>, Nagarjuna Narala <sup>1</sup>, Sagar Narala <sup>1</sup>, Sivaram Munnangi <sup>1</sup>,  
Sateesh Kumar Vemula <sup>1,2</sup> and Michael Repka <sup>1,3,\*</sup>

<sup>1</sup> Department of Pharmaceutics and Drug Delivery, School of Pharmacy, University of Mississippi, University, MS 38677, USA

<sup>2</sup> Department of Pharmaceutics, School of Pharmaceutical Sciences, Lovely Professional University, Phagwara, Punjab 144001, India

<sup>3</sup> Pii Centre for Pharmaceutical Technology, School of Pharmacy, University of Mississippi, University, MS 38677, USA

\* Correspondence: marepka@olemiss.edu; Tel.: +1 662 915 1155; fax: +1 662 915 1177

**Abstract:** Hypertension (HTN) is the foremost contributor to cardiovascular diseases (CVD), which remain a leading cause of death. However, adherence to the properly prescribed dosage form is critical and challenging for patients with chronic diseases such as HTN to prevent illness progression and death. The study's objective was to develop AMB-loaded subcutaneous implants to reduce the frequency of administration, thus improving patient compliance during HTN management. AMB subcutaneous implants were prepared using continuous hot melt extrusion technology using PCL and PLGA with dimensions of 7.5 cm (length) by 2 mm (diameter). The implants were characterized for thermal characteristics, drug-excipient incompatibilities, surface morphology, fracturability, in vitro release, and stability studies. DSC showed that the drug was in the crystalline state in the fabricated implants. Scanning Electron Microscopy (SEM) revealed a smooth surface. The lead formulation presented good drug content, showed an extended drug release profile over 30 days, and followed zero-order release kinetics with a mean dissolution time of 15 days. The formulation was stable over 30 days in accelerated stability conditions (the last time point was tested, 40°C/75% RH), and the release profile was similar to the initial drug release profile. The lead formulation showed good fracturability during textural analysis. Therefore, the hot melt extruded implants could be an alternative management strategy for conventional amlodipine besylate (AMB) formulation.

**Keywords:** hypertension; subcutaneous implants; hot melt extrusion; controlled drug delivery; biodegradable; implantable drug delivery

## 1. Introduction

Cardiovascular diseases (CVD), a significant global cause of mortality, include hypertension as a leading factor in early deaths worldwide [1]. Projections indicate that by 2025, approximately 1.56 billion adults will suffer from hypertension [2]. High blood pressure, also referred to as hypertension, is diagnosed when the systolic blood pressure (SBP) registers at 140 mmHg or higher and/or the diastolic blood pressure (DBP) exceeds 90 mmHg [3]. It is often known that one of the main risk factors for cardiovascular disease is hypertension [4].

Amlodipine Besylate (AMB) is a long-acting, lipophilic, third-generation dihydropyridine, calcium channel blocker used to treat hypertension, angina, and coronary artery disease. It acts through calcium influx inhibition into vascular smooth muscle cells and myocardial cells, causing a decrease in peripheral vascular resistance. The most recent calcium channel blockers, like felodipine, nisoldipine, dihydropyridines, and AD (Amlodipine), have better vascular selectivity and longer

half-lives. The gradual and consistent attachment to target receptors leads to a seamless initiation of action, ensuring effective blood pressure control for a continuous 24-hour period [5]. Calcium Channel Blockers (CCB's) are still used as monotherapy options because drugs such as amlodipine have shown superior efficacy as monotherapy and combined with angiotensin converting enzyme (ACE) inhibitors for decreasing cardiovascular events in high-risk hypertensive patients, with excellent tolerability [6].

While oral solid formulations are readily accessible in the market, they present several hindrances, including challenges associated with tablet administration in geriatric patients and the potential for unintentional medication omission due to underlying medical conditions. Consequently, there is a dire need to develop an extended-release dosage form capable of alleviating these challenges. Formulations such as subcutaneous implant-based drug delivery systems represent a promising solution.

The current study chose Poly(caprolactone) PCL and PLGA Poly (lactic-co-glycolic acid) for fabricating implants. These polymers are well-established and widely utilized in implant technology because of their biocompatible, biodegradable, and good mechanical strength properties [7]. The advantage of biodegradable implants is that they do not need to be removed from the patient's body after insertion. They break into small fragments, eventually excreted or absorbed by the body [8,9]. An implantable drug delivery system [IDDS] allows targeted and localized drug delivery and may achieve a therapeutic effect with a lower drug concentration [10,11]. Subcutaneous implants are placed into the subcutaneous tissue beneath the hypodermis region of the skin using a hypodermic needle, injection, or minor surgery [12]. Subcutaneous implants currently available in the market are Norplant-II, Viadur, and Ozurdex [13].

Various methods are available for implant fabrication, such as Compression molding, Injection molding, 3D printing/ Additive Manufacturing (AM), and Hot Melt Extrusion [14,15]. Hot-melt extrusion (HME) was expanded to the pharmaceutical industry in the 1970s. It was used in formulation, product development, and manufacturing [16]. It is more affordable, does not require solvents, and can be produced more continuously than other methods; hot-melt extrusion has become a leading manufacturing technology for the pharmaceutical industry [17]. HME has been significantly used in fabricating various polymeric implants and novel drug delivery systems [18].

Among various techniques, hot-melt extrusion is a well-established and highly efficient technology particularly suited for large-scale production [19]. It facilitates continuous manufacturing, minimizing waste and yielding high-quality results. It has previously been shown that HME is a reliable, cutting-edge method for creating solid dispersions that enable targeted, modified, prolonged, and time-controlled drug administration [20]. In the typical HME process, a single-screw or twin-screw apparatus rotates either in a clockwise (co-rotating) or anticlockwise (counter-rotating) direction. This rotation propels the Active Pharmaceutical Ingredient (API) and polymer towards a die under elevated temperature and pressure, producing uniform drug-loaded filaments. HMEs can create precisely controlled temperature and pressure conditions within the barrel, ensuring the materials melt above their respective melting and/or glass transition temperatures. The molecular mixing essential for the process occurs through screw shearing [21]. Once extruded, the materials take on solid filament or granule forms. This process demonstrates remarkable efficiency and operates continuously, making it a favored choice for various manufacturing needs [22]. The current study used a HAAKE Mini Lab twin-screw extruder with pneumatic feeding to fabricate subcutaneous implants.

The current study was designed to develop a novel Polycaprolactone, Poly (lactic-glycolic acid) and Amlodipine Besylate based subcutaneous implant using a continuous manufacturing process (hot-melt extrusion) for extended release of AMB as an alternative management strategy for hypertension, while overcoming issues such as: - missing medication, swallowing tablets which are associated with oral solid dosage forms of amlodipine besylate. This is the first study involving Amlodipine Besylate coupled with Hot Melt Extrusion and evaluating and characterizing the subcutaneous implants for treating hypertension.

2. Materials and Methods

2.1. Materials

Amlodipine Besylate was purchased from Ria International LLC (East Hanover, N.J., USA). Polycaprolactone (PCL) (Mw- 80,000) was purchased from Sigma Aldrich Inc (Milwaukee, Wisconsin, USA), and Poly-Lactic-glycolic acid (PLGA) (Resomer LG 855 S, ester terminated, lactide) with PLA: PGA (Polylactic acid: Polyglycolic acid) ratio 85:15 was purchased from Sigma Aldrich Inc (St Louis, M.O, USA). All other chemicals were of analytical grade.

2.2. Solvent Evaporation for the Fabrication of Uniform Filaments

The drug and polymer (PCL or PLGA) were weighed in different ratios and dissolved in a beaker containing chloroform using a magnetic stirrer. Subsequently, the solution was transferred to a petri dish and placed in a fume hood for 24 to 48 hours to facilitate solidification and solvent evaporation. The solidified material was cut into small pieces and used for extrusion through HME to fabricate implants.

2.3. Preparation of Implants with Hot Melt Extrusion

A HAAKE Minilab Lab extruder (Thermo Scientific, Waltham, MA, USA) was used to extrude implants. The solvent-evaporated mixture of the drug (AMB) and polymers (Poly Caprolactone, PCL, and Poly lactic-glycolic acid, PLGA) were cut into small pieces and manually fed into the extruder. The implants were extruded at a temperature of 90°C and a screw speed of 25 rpm, utilizing a 2 mm die for the extrusion. Following extrusion, the resulting filaments were allowed to cool and then cut to a length determined by the drug loadings. Subsequently, the extrudates were characterized for drug content and drug release, tensile strength, FTIR, SEM, DSC, and stability.

2.4. Formulation Composition

The formulations were designed to deliver 2.5 mg of AMB daily. Polycaprolactone and Poly-glycol-lactide acid were used for the controlled drug release of AMB. Table 1 denotes different compositions of prepared formulations.

Table 1. Composition of Amlodipine Besylate in Implants.

Formulations (%w/w)	Amlodipine Besylate (AMB)	Polycaprolactone (PCL)	Poly Lactic- glycolic acid (PLGA)	Solvent Casting Performed
F1	20	80	00	No
F2	35	65	00	No
F3	50	50	00	No
F4	20	80	00	Yes
F5	35	65	00	Yes
F6	50	50	00	Yes
F7	65	35	00	Yes
F8	50	00	50	Yes
F9	50	25	25	Yes

## 2.5. Characterization of Implants

### 2.5.1. Tensile Strength Analysis of Implants

The extruded implants were analyzed for their strength and flexibility to ensure they could be used for surgical implantation. The test used the TA-XT2i Texture Analyzer (Stable Micro Systems Ltd., Godalming, England) equipped with a TA-92 adjustable 3 pt bend/snap fixture module. The test was performed using the following parameters: the gap between the clamps - 10 mm; pre-test speed - 2 mm/s; test speed - 2 mm/s; post-test speed - 10 mm/s; probe moving distance - 10 mm. The extruded filaments were placed on the sample support clamps while a 3 mm thick rounded end, bell lock-shaped knife was attached to the holder at the texture analyzer's upper part. The blades traversed 10 mm from their initial position until they reached the filament's vicinity. Exponent version 6.1.5.0 software (Stable Micro Systems Ltd., Godalming, UK) was used to monitor and plot the resistance force over the distance (or time). The test was carried out thrice on each filament [23].

### 2.5.2. Differential Scanning Calorimetry

Pure samples of the drug (Amlodipine Besylate), polymers (PCL and PLGA), physical mixture (Amlodipine Besylate, PCL, and PLGA), and extruded formulations were analyzed with the help of Discovery 25 differential scanning calorimeter (TA Instruments, Newcastle, DE, USA) combined with an RCS90 refrigerator cooling system. T-zero aluminum pans consisting of the samples (5-10 mg) were tightly sealed with aluminum pans. The parameters for the testing involve a heating rate of 10°C/min from 0 to 250°C, conducted in a nitrogen atmosphere with a base purge flow of 50 mL/min [24].

### 2.5.3. FTIR Analysis

The pure drug, polymers, and extruded filaments were analyzed for infrared spectra with the help of Cary 660 FTIR spectrophotometer (Agilent Technologies, Santa Clara, California, USA) combined with ATR apparatus (Pike Technologies MIRacle, Madison, WI, USA) attached with single bounce made up of diamond coated ZnSe internal reflection element. A spectrum of 4000-650 cm<sup>-1</sup> was recorded with 32 scans [25].

### 2.5.4. Scanning Electron Microscopy (SEM) Analysis

SEM analysis was performed to evaluate the surface morphologies of pure drugs, polymers, and fabricated implants through a JSM-7200FLV (JEOL, Peabody, MA, USA) scanning electron microscope with an accelerating voltage of 5kV. Double-adhesive tape was used to adhere all the samples over the SEM stubs. All the samples were sputter-coated with platinum and were kept in an argon atmosphere. The Denton Desk V TSC sputter coater (Denton Vacuum, Moorestown, NJ, USA) was used to sputter-coat all the samples before imaging [26].

### 2.5.5. Content Uniformity

Content Uniformity was performed to confirm the uniform distribution of Amlodipine Besylate in the filament. The implants were randomly selected from each batch, weighed, cut into 3 sections (first, middle, and last), and then transferred to 20 mL scintillation vials dissolved in THF. The solution was diluted with THF-Water mixture, and the resulting solution was analyzed for Amlodipine Besylate content in UV-Vis spectroscopy at 239 nm. The test was performed to confirm that a dose of 2.5 mg was available in the three sections of the filaments.

### 2.5.6. Solubility Studies

Solubility studies were performed to determine the saturation solubility of the AMB in buffer media used for drug release studies (Phosphate Buffer pH 7.4 with 0.1%, 0.5%, or 1.0% Tween 80). Amlodipine Besylate was weighed and dissolved in different concentrations of Tween 80 to check



the solubility of the drug in the buffer in a bio shaker at 400 rpm. The experiments were performed for 48 hours, and samples were analyzed at 24-hour intervals. The samples were collected with the help of a 0.45  $\mu\text{m}$  nylon filter attached to the syringe. The collected samples were analyzed with a UV-Vis Spectrophotometer at 239 nm.

2.5.7. In-vitro drug release study of AMB-loaded implants

The in-vitro release study of Amlodipine Besylate implants was performed in a horizontal water bath shaker at  $37 \pm 2^\circ\text{C}$  in pH 7.4 Phosphate buffer with surfactant (1% Tween 80). The drug release study was performed for the drug-loaded implants over 30 days. The horizontal water bath shaker was set to move horizontally at 100 rpm to ensure the media had uniform mixing. The samples ( $n=3$ ) were kept in 50 mL scintillation vials containing a 30 mL dissolution media volume. The whole media (30 mL) was replaced with fresh buffer every 24 h, and collected samples were analyzed. The samples were analyzed by UV-Vis spectroscopy at 239 nm.

2.5.8. Release Kinetics of AMB and Mechanism

The release kinetics of the formulations were performed to study the mechanism of drug release from the fabricated implants; the generated data was evaluated for release kinetics with the help of the following equations in Table 2.

Table 1. Mathematical Modelling and Equation for Deriving Release Kinetics.

Mathematical Model	Equations
Zero-order	$Q_0 - Q = kt$
First-order	$\ln Q = kt$
Higuchi's matrix	$Q_0 - Q = kt^{1/2}$
Korsmeyer- Peppas	$\text{Log } (Q_0 - Q) = n \log t + \log k$

Where  $Q_0$  and  $Q$  are initial drug content at time  $t_0$  and drug content at time  $t$ , respectively; Zero-order model: % drug released vs. time; First-order model:  $\ln$  amount drug remaining vs. time; Higuchi model: % drug released vs. square root of time; Korsmeyer-Peppas model:  $\log$  % drug released vs.  $\log$  time [27].

2.5.9. Stability Studies

The stability studies were performed for 30 days. The samples were kept in a Caron 6030 stability chamber at  $40^\circ\text{C}/75\% \text{ RH}$  for accelerated storage. The samples were collected on days 15 and 30 at different time intervals and analyzed for DSC, drug content, and drug release profile. The samples obtained from assay and drug release were analyzed with UV-Vis spectroscopy at 239 nm [28].

3. Results

3.1. Solvent Evaporation and Hot Melt Extrusion

Initially, an 11 mm twin screw extruder was used for the fabrication. Unfortunately, despite undergoing two extrusion cycles, content uniformity was not achieved. This might be because of the pellet nature of polymers, which are hard to crush. PCL and PLGA were freeze-dried and sized with dry ice. PCL pellets turned into chips/flakes, while PLGA crystals were too elastic to crush in a pestle and mortar. Consequently, this non-uniform physical mixture hinders both content uniformity and the quality of the extruded product.

Subsequently, a Minilab extruder was employed for filament fabrication using the direct extrusion method. While the extrudates were successfully produced, they did not meet the content uniformity. Consequently, by the previously described procedure, the product obtained through the solvent evaporation technique was utilized for filament extrusion. This approach resulted in extrudates within the specified content uniformity limits with minimal variability. The principal

benefit of conducting solvent evaporation lies in the consistent blending of drug and polymer at the molecular level, as they exist in a solution state before being placed within a fume hood.

### 3.2. Tensile Strength Analysis of Implants

Repka-Zhang Test, also known as the 3-point bend test, was carried out to evaluate the properties of the extruded filaments. The filaments should have enough strength and good flexibility because they are administered in an area susceptible to movement, and a brittle filament could break during the administration or treatment process. Tensile strength and uniform strain. The physical strength analysis of F6, F8, and F9 are presented in Table 2. The F8 formulation, when tested, showed characteristics of brittleness in terms of hardness, fracture ability, and stress.

On the other hand, the F6 and F9 formulations displayed improved properties in terms of hardness, fracturability, and stress tolerance. This indicates that these formulations were more resistant to breaking and had better overall strength. Of particular note is the F9 formulation, which did not fracture during the entire testing process. This suggests that PCL (polycaprolactone) acted as a plasticizer in the filament contributed to its flexibility and overall strength. The tests for the F6 and F9 formulations were terminated because these formulations did not break under the applied forces. This indicates that they exhibited exceptional strength and durability, surpassing the limits of the testing equipment. Formulations F4, F5, and F7 drug release profiles were not constant, and significant fluctuation was seen. Hence, the above formulations were not considered for further chemical and physical analysis.

**Table 2.** Texture Analysis of F 6, F 8, and F 9 Formulations.

Samples	Hardness (g)	Fracturability (mm)	Stress (g/mm <sup>2</sup> )
F6 (PCL)*	5315.54 ± 26.99	31.4 ± 0.0047	1082.87 ± 5.49
F8 (PLGA)	716.77 ± 8.78	59.55 ± 2.32	-0.00967 ± 0.01
F9 (PCL+PLGA)*	5484.45 ± 182.41	21.46 ± 1.30	1117.28 ± 37.16

\* Formulations F6 and F9 did not break till the end of the experiment into 2 or more pieces when force was applied.

### 3.3. Differential Scanning Calorimetry

Differential Scanning Calorimetry (Thermal Analysis) determined the formulation ingredients' physical state (crystalline or amorphous). Pure AMB, PCL, PLGA, physical mixtures, and formulations (F6, F8, and F9) were examined for their physical state. Figure 1 shows all obtained DSC thermograms. AMB showed a sharp endothermic melting peak at 207.43°C [29]. Previous experiments demonstrated the melting point range 197-206°C [30], while Silva, A.C.M., et al. found an endothermic peak at 207°C [31]. PCL showed a sharp endothermic peak at 61.59°C; several experiments have reported similar values [32,33], and PLGA showed broad endothermic peaks at 166.72°C [34]. The physical mixture of F6 and its corresponding formulation showed 2 endothermic peaks at ~ 207.4 and 60.71°C for AMB and PCL, respectively. At the same time, the Physical Mixture of F8 and its corresponding formulation showed 2 endothermic peaks at ~ 206.46 and 165.265°C for AMB and PLGA, respectively. Physical Mixtures of F9 and its corresponding formulation showed 3 endothermic peaks at ~ 207.125, 60.03, and 165.17°C for AMB, PCL, and PLGA, respectively. F6, F8, and F9 implants showed smaller drug peaks compared to pure drugs; the F6 formulation showed the smallest, while F8 showed the highest. These results confirm that AMB was partially converted to an amorphous form during extrusion.

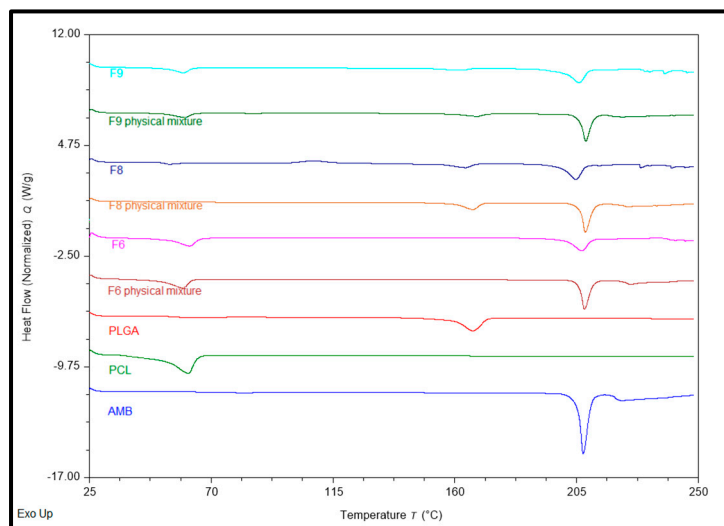


**Figure 1.** DSC thermograms of Pure Drug, Polymers, Physical Mixtures, and corresponding formulations.

### 3.4. FTIR Spectroscopy

FTIR was performed to confirm that the drug and polymer are compatible in all formulations. The FTIR spectra of Pure AMB, PCL, and PLGA were used as a reference for analyzing the FTIR spectra of implants that consist of the same materials. Figure 2 shows the FTIR spectra of the pure drug, polymers, and their formulations. Pure AMB exhibited IR spectra peaks at  $3305\text{ cm}^{-1}$ , associated with the N-H stretching bond. Also, distinctive peaks at  $1675$  and  $1614\text{ cm}^{-1}$  corresponded to C=O groups from ethyl ester and methyl ester side chains.

Further peaks at  $1432$  and  $1267\text{ cm}^{-1}$  are attributed to C=C and C-O stretching vibrations, respectively [35,36]. The PCL showed peaks at  $2949\text{ cm}^{-1}$  and  $2865\text{ cm}^{-1}$  [37], which are associated with the asymmetric and symmetric  $\text{CH}_2$  group stretching, alongside a sharp band at  $1727\text{ cm}^{-1}$  was observed related to the carbonyl group stretching in the polymer [38]. At the same time, the PLGA showed an intense peak in a region between  $1770$  and  $1750\text{ cm}^{-1}$ , which is associated with the stretching vibration of carbonyl groups from two monomers [39]. Additionally, moderate peaks observed between  $1300$  and  $1150\text{ cm}^{-1}$  are associated with asymmetric and symmetric C-C(=O)-O stretches, which are characteristics of esters in this spectral region [40]. All the characteristic peaks of AMB, PCL, and PLGA are present in the IR spectra of the formulations, indicating no formation of additional peaks. Thus, there is no chemical interaction between AMB and polymers.



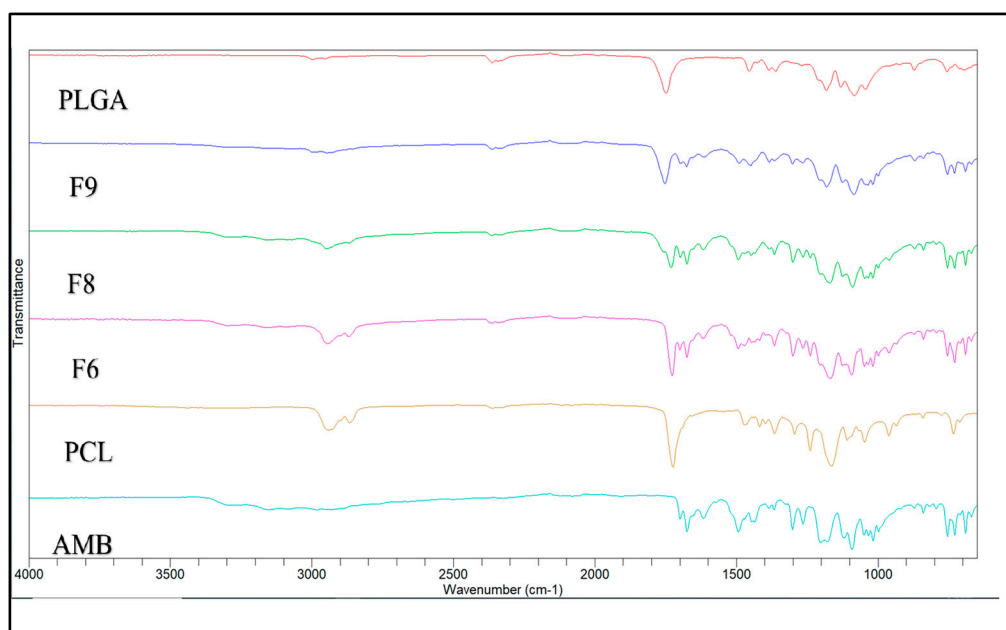


**Figure 2.** FTIR spectra of Pure AMB, Polymers, and Corresponding Formulations.

### 3.5. Scanning Electron Microscopy (SEM)

A smooth surface is a critical parameter as it is a crucial indicator of successful implant fabrication. This is crucial because a rough surface may induce irritation at the site of application. Figure 3 presents SEM images depicting the surface morphology following implant fabrication. Notably, formulations F6 and F9 exhibited exceptionally smooth surfaces without any visible crystals, even under magnifications of up to 30x and 50x, respectively. Formulations with PCL and drug have shown smooth surfaces, free from pores in previous experiments, similar to the F6 formulation [41].

In contrast, some experiments with a combination of PCL/PLGA found smooth surface morphology similar to the above F9 formulation [42]. Meanwhile, formulation F8 showed a rough surface at 30x and 50x. The rough surface on F8 could be attributed to the presence of AMB; He et al. found a similar rough surface on doxorubicin-loaded implants with PLGA [43].

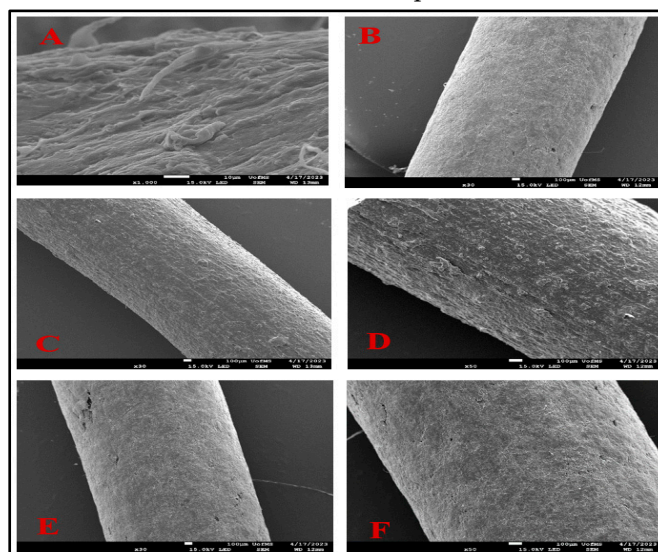


**Figure 3.** Scanning Electron Microscopy analysis of A (AMB), B (F6), C (F8 at 30x), D (F8 at 50x), E (F9 at 30x), F (F9 at 50x).

### 3.6. Content Uniformity

Drug Content Uniformity was performed to confirm the content uniformity of the AMB in the implants. The content uniformity of all the formulations is shown in Table 3. The Standard deviations of F4, F5, F6, F8, and F9 were less than 5 while F1, F2, and F3 showed standard deviations of more than 5%. Hence, the formulation F4 – F9 were within in acceptable limits of content uniformity.

**Table 3.** Content Uniformity of Amlodipine Besylate in Implants.

Formulations	Content Uniformity (%)
F1	55.3±20.62
F2	73.4±21.8
F3	71.0±27.10
F4	98.5±3.3
F5	105.1±2.60
F6	99.9±2.64
F7	96.9±2.63
F8	97.0±3.05
F9	102.2±2.18

### 3.7. Solubility Studies

Solubility studies revealed that the drug exhibited its highest solubility in phosphate buffer (pH 7.4) containing 1% Tween 80, yielding a 5.02 mg/mL concentration. In contrast, it displayed the lowest solubility with a concentration of 0.79 mg/mL in a solution containing 0.1% Tween 80, which was evident because of the low surfactant concentration. A significant increase in AMB solubility was observed when comparing 1% (5.02 mg/mL) Tween 80 to 0.5% Tween 80 (2.95 mg/mL). Consequently, the analysis concluded that a 1% concentration of Tween 80 would be the most suitable choice for the dissolution studies. Table 4 shows the drug solubility of AMB.

**Table 4.** Solubility Studies of AMB.

Sample	AMB Solubility (mg/mL)
AMB+Phosphate buffer	0.26
AMB + Phosphate buffer + Tween 80 (0.1%)	0.79
AMB + Phosphate buffer + Tween 80 (0.5%)	2.95
AMB + Phosphate buffer + Tween 80 (1.0%)	5.02

### 3.8. In-vitro release of AMB from Implants

The drug release profiles of all the formulations are depicted in Figure 4 (a). The formulations F6, F8, and F9 were selected because they could release the drug close to the target daily dose of 2.5 mg. The formulations F4 and F5 exhibited an average daily drug release of ~ 0.62 mg and 1.14mg daily for 15 days. However, these formulations displayed inconsistent drug release patterns. They were not able to achieve the targeted drug release due to their low drug content and high polymer concentration, which hindered drug release. The F7 formulation released ~1.61 mg of the drug daily for 15 days but exhibited significant fluctuations in daily AMB release. This could be attributed to the high drug load, which overshadowed the controlled release property of PCL in the formulation.

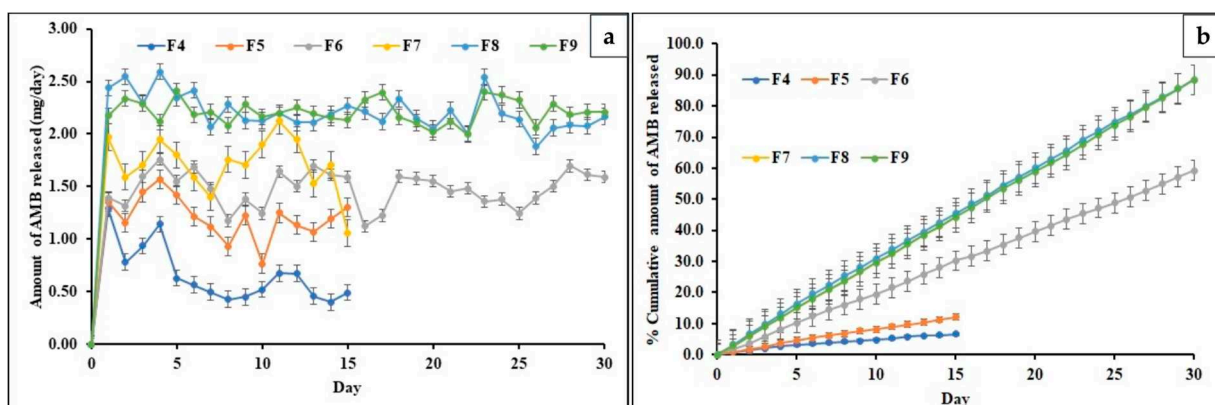


**Figure 4.** a) Per day AMB Release of all Formulations, b) Cumulative Drug Release of AMB of all Formulations.

Consequently, the study for formulations F4, F5, and F7 was terminated after 15 days due to their inability to deliver the targeted drug quantity. In addition, F6, F8, and F9 implants showed an average daily drug release of  $\sim 1.56$ ,  $2.47$ , and  $2.25$  mg in 30 days. The formulation F6 could not release the targeted daily dose, which could be because of the presence of a high concentration of hydrophobic PCL [44].

On the contrary, the release from the F8 formulation was consistent and achieved the targeted daily dose. This might be because F8 is composed of PLGA, resulting in accelerated drug release compared to F6. The F9 formulation was able to release the targeted dose constantly. This result may be due to the interplay between PCL's hydrophobic nature and PLGA's relatively lower hydrophobicity than PCL, which balanced and facilitated the targeted drug release. Incorporating PLGA into the PCL matrix led to an increased degradation rate, resulting in the release of a higher drug quantity than other formulations [45].

### 3.9. Release Kinetics

Mathematical modeling was performed to find the release pattern from the formulations. The model which depicted the highest  $R^2$  value was considered the best model to describe the release kinetics. Considering the per day release of AMB, Formulations F6, F8, and F9 are discussed in the release kinetics, while the rest are depicted in Table 5. The highest coefficient of determination ( $R^2$ ) is mentioned in Table 5. All formulations' highest coefficient of determination ( $R^2$ ) was observed for zero-order release. F6 showed the highest value of the coefficient of determination for zero-order release ( $R^2$ - 0.9997), followed by Higuchi ( $R^2$ - 0.9401), Korsmeyer-Peppas model ( $R^2$ - 0.9176), and First-order ( $R^2$ - 0.7964). F8 showed the highest value of the coefficient of determination for zero-order release ( $R^2$ - 0.9997), followed by the Korsmeyer-Peppas model ( $R^2$ - 0.9591), Higuchi ( $R^2$ - 0.9396), and First- order ( $R^2$ - 0.76). F9 showed the highest value of the coefficient of determination for zero-order release ( $R^2$ - 0.9999), followed by the Korsmeyer-Peppas model ( $R^2$ - 0.9495), Higuchi ( $R^2$ - 0.9403), and First- order ( $R^2$ - 0.7739). The release exponent values ( $n$ ) of formulations F6, F8, and F9 were 0.433, 0.3097, and 0.3509, respectively.

Mean dissolution time was calculated to analyze the time (in days) required for the formulation to dissolve in the dissolution media. Table 5 depicts the mean dissolution time of all the formulations. Considering the per-day release of formulations, F6, F8, and F9 are discussed, while the rest are represented in Table 5. Formulations F6, F8, and F9 showed a mean dissolution time (MDT) of 15, 14.64, and 14.96 days, respectively.

**Table 5.** Mathematical modelling, release kinetics, and mean dissolution time of F4, F5, F6, F7, F8, and F9 formulations.

Formulations	Zero Order		First Order		Higuchi Model		Korsmeyer–Peppas model			Mean
	Release		Release							Dissolution
	R <sup>2</sup>	K	R <sup>2</sup>	K	R <sup>2</sup>	K	R <sup>2</sup>	n	K	Time (days)
F4	0.9786	0.0174	0.8764	0.0023	0.9767	0.3743	0.7506	0.271	0.3853	6.2
F5	0.9965	0.033	0.8777	0.003	0.9459	0.6911	0.7508	0.3023	0.4752	7.22
F6	0.9997	0.0818	0.7964	0.0018	0.9401	8.7343	0.9176	0.433	0.7408	15
F7	0.9991	0.0968	0.8364	0.0035	0.9267	2.0047	0.922	0.233	0.6533	7.31
F8	0.9997	0.122	0.76	0.0018	0.9396	10.793	0.9591	0.3097	0.7673	14.64
F9	0.9999	0.1225	0.7739	0.0018	0.9403	10.726	0.9495	0.3509	0.7781	14.96

Table 6 depicts the time to release 10, 50, and 80% of the drug from formulations, while Figure 4(b) depicts the cumulative drug release of AMB for all formulations. Regarding per-day release, Formulations F6, F8, and F9 are also discussed in the release. F6 took the 6th day to reach 10% of drug release, while 50% of the drug was released on the 25th day. The formulation could not release 80% of the drug during the study because of the hydrophobic nature of PCL. F8 took the 4<sup>th</sup> day to reach 10% of drug release, while 50% was attained on the 17th day and 80% on the 27<sup>th</sup> day of the release study. However, F9 released 10% of the drug on the 3rd day, 50% of the drug on the 18<sup>th</sup> day, and 80% of the drug was released on the 28th of the release study, depicted in Figure 4 (b).

**Table 6.** Days to Release 10, 50, and 80% of AMB.

Formulations	T10 %	T50 %	T80 %
F4	NA	NA	NA
F5	14	NA	NA
F6	6	25	NA
F7	4	NA	NA
F8	4	17	27
F9	3	18	28

### 3.9.1. Stability Studies

The physicochemical stability of AMB-loaded implants was evaluated in a stability chamber at 40°C/75 RH on the 15<sup>th</sup> (first-time point tested) and 30<sup>th</sup> day (last-time point tested). No physical changes in color and texture were observed during the stability period. The effect of storage conditions on F6 concerning assay at Day 1, Day 15, and Day 30 were 102.3, 99.1 and 97.3%, respectively; F8 showed assay 100.1, 97.2 and 96.1%, respectively, while F9 showed assay of 99.3, 98.8 and 979.9% at Day 1, Day 15 and Day 30 respectively. The formulations showed no significant change in drug content under the storage conditions over 30 days. The effect on thermal behavior was conducted on Days 1, 15, and 30 and is shown in Figure 5. F6 on Day 1 showed a peak at 60.71 and 207.4°C for PCL and AMB, F6 showed an endothermic peak at 65.26 and 208.70°C for PCL and AMB on Day 15 of the test and showed an endothermic peak at 66.90 and 206.83°C for PCL and AMB. F9 showed an endothermic peak at 59.77, 161.96, and 205.87°C for PCL, PLGA, and AMB, while an endothermic peak was observed at 65.10, 162.06, and 209.72°C for PCL, PLGA, and AMB. Endothermic peaks were observed at 65.61, 162.35, and 207.57°C for PCL, PLGA, and AMB for F9. While F8 on day 1 showed an endothermic peak at 206.46 and 165.265 for AMB and PLGA, and on day 15<sup>th</sup>, it depicted an endothermic peak at 208.15 and 164.33°C for AMB and PLGA, it showed a peak at 61.83°C, which might be the polymer's glass transition temperature in the formulation, according to Liu [46]. Another exothermic peak at 116.74°C was not expected. An endothermic peak

at 164.74, 205.64°C for PLGA and AMB was observed; it showed another peak at 60.10°C, which might be the polymer's glass transition temperature in the formulation, according to Liu [46]. A similar exothermic peak was observed at 110.92°C, which was not expected. There was no justification for the above exothermic peak during our literature search. Hence, F8 was not selected as our lead formulation.

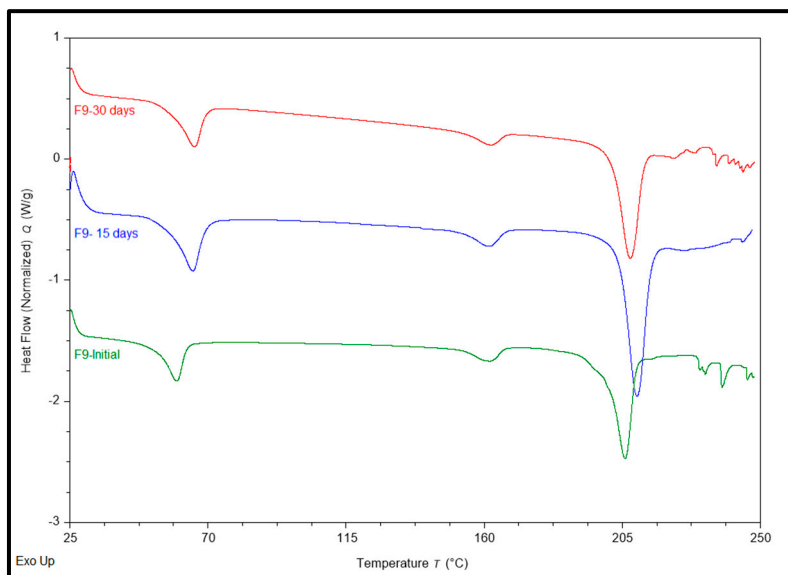


**Figure 5.** DSC thermograms of F9 formulations over initial, 15- and 30-day period.

### 3.9.2. In vitro release study of implants after stability studies

The study was performed for 15 days for F6, F8, and F9 formulations (Figure 6); it was performed after 30 days to confirm the efficacy and stability of the formulations during the experiment. The in-vitro release studies were performed in a 30 mL dissolution media (pH 7.4 Phosphate buffer) in a horizontal bath shaker at 100 rpm and 37°C. F9 formulation over 15 days showed an average daily drug release of ~2.21 mg. The drug release profile of the formulation F9 (Stability Studies) was similar to the initial drug release profile of the same formulation. Hence, the lead formulation F9 showed optimum drug release with no signs of atypical behavior and was stable for 30 days.

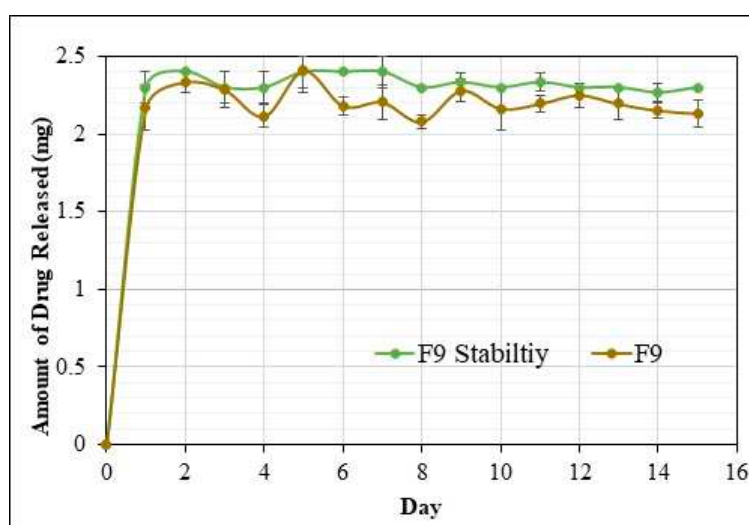


**Figure 6.** Per day AMB release of F9 formulations after stability studies over 15 days.



#### 4. Conclusion

AMB-loaded implants were successfully prepared with PCL and PLGA using hot melt extrusion. The physicochemical properties of implants were evaluated using DSC, FTIR, SEM, texture analyzer, stability, and in-vitro drug release studies. The lead formulation (F9) showed a smooth, uniform, homogenous surface in SEM and good fracturability and hardness in the texture analyzer. The lead formulation was also stable during the testing period and showed an extended drug release profile for 15 days. F9 followed a zero-order release kinetics with an  $R^2$  of 0.9999 and a mean dissolution time of 14.96 days. Future studies concerning performing release profiles for a more extended period and pharmacokinetics in animal models are additional studies required to develop the formulation into the commercial dosage form. In conclusion, the fabricated implants under this investigation could serve as an alternative drug delivery platform for the conventional AMB oral dosage forms for better therapeutic outcomes.

**Supplementary Materials:** The following supporting information can be downloaded at the website of this paper posted on Preprints.org.

**Author Contributions:** Conceptualization, K.C, N.N and S.N; methodology, validation, formal analysis, investigation, data curation, KC, N.N, S.N and S.M; writing—original draft preparation, K.C, N.N, S.N, S.M; writing—review and editing, S.K.V and M.A.R; supervision, M.A.R.

**Data Availability Statement:** The data presented in this study are available within the article and supplementary material.

**Acknowledgments:** Scanning Electron Microscopy images presented in this work were generated using the instruments and services at the Microscopy and Imaging Centre at the University of Mississippi. This facility is partly supported by grant 1726880, from the National Science Foundation.

**Conflicts of Interest:** The authors declare no conflicts of interest.

#### References

1. Whelton, P.K. Epidemiology of Hypertension. *Lancet* 1994, 344, 101–106, doi:10.1016/s0140-6736(94)91285-8.
2. Lago, R.M.; Singh, P.P.; Nesto, R.W. Diabetes and Hypertension. *Nat Rev Endocrinol* 2007, 3, 667–667, doi:10.1038/ncpendmet0638.
3. Sherwood, A.; Carels, R.A. Blood Pressure. In *Encyclopaedia of Stress* (Second Edition); Fink, G., Ed.; Academic Press: New York, USA 2007; pp. 335–342.
4. Fares, H.; DiNicolantonio, J.J.; O'Keefe, J.H.; Lavie, C.J. Amlodipine in Hypertension: A First-Line Agent with Efficacy for Improving Blood Pressure and Patient Outcomes. *Open Heart*. 2016 Sep 28;3(2): e000473. doi: 10.1136/openhrt-2016-000473.
5. Sheraz, M.A.; Ahsan, S.F.; Khan, M.F.; Ahmed, S.; Ahmad, I. Formulations of Amlodipine: A Review. *J Pharm (Cairo)* 2016, 2016, 8961621, doi:10.1155/2016/8961621.
6. Tripathi, K.D. *Essentials of Medical Pharmacology*; JP Medical Ltd., New Delhi, India 2013; pp. 604–620.
7. Deng, S.; Chen, A.; Chen, W.; Lai, J.; Pei, Y.; Wen, J.; Yang, C.; Luo, J.; Zhang, J.; Lei, C.; et al. Fabrication of Biodegradable and Biocompatible Functional Polymers for Anti-Infection and Augmenting Wound Repair. *Polymers (Basel)* 2022, 15, 120, doi:10.3390/polym15010120.
8. Makadia, H.K.; Siegel, S.J. Poly Lactic-Co-Glycolic Acid (PLGA) as Biodegradable Controlled Drug Delivery Carrier. *Polymers* 2011, 3, 1377–1397, doi: 10.3390/polym3031377.
9. Manoukian, O.S.; Arul, M.R.; Sardashti, N.; Stedman, T.; James, R.; Rudraiah, S.; Kumbar, S.G. Biodegradable Polymeric Injectable Implants for Long-Term Delivery of Contraceptive Drugs. *Journal of applied polymer science* 2018, 135, 46068, doi: 10.1002/app.46068.
10. Dash, A.; Cudworth, G. Therapeutic Applications of Implantable Drug Delivery Systems. *Journal of Pharmacological and Toxicological Methods* 1998, 40, 1–12, doi:10.1016/S1056-8719(98)00027-6.
11. Kleiner, L.W.; Wright, J.C.; Wang, Y. Evolution of Implantable and Insertable Drug Delivery Systems. *Journal of Controlled Release* 2014, 181, 1–10, doi:10.1016/j.jconrel.2014.02.006.
12. Kim, H.; Park, H.; Lee, S.J. Effective Method for Drug Injection into Subcutaneous Tissue. *Sci Rep* 2017, 7, 9613, doi:10.1038/s41598-017-10110-w.

13. Simpson, S.M.; Widanapathirana, L.; Su, J.T.; Sung, S.; Watrous, D.; Qiu, J.; Pearson, E.; Evanoff, A.; Karunakaran, D.; Chacon, J.E.; et al. Design of a Drug-Eluting Subcutaneous Implant of the Antiretroviral Tenofovir Alafenamide Fumarate. *Pharm Res* 2020, 37, 83, doi:10.1007/s11095-020-2777-2.
14. Iyer, S.S.; Barr, W.H.; Karnes, H.T. Profiling in Vitro Drug Release from Subcutaneous Implants: A Review of Current Status and Potential Implications on Drug Product Development. *Biopharmaceutics & Drug Disposition* 2006, 27, 157–170, doi:10.1002/bdd.493.
15. Ganesh, K.; Yang, S.; Schillace, S.; Vita, V.; Wang, Y.; Ehmann, K.F.; Guo, P. A Review of Manufacturing Techniques for Subcutaneous Drug Delivery Implants. *Procedia CIRP* 2022, 110, 329–334, doi.org/10.1016/j.procir.2022.06.059
16. Patil, H.; Tiwari, R.V.; Repka, M.A. Hot-Melt Extrusion: From Theory to Application in Pharmaceutical Formulation. *Aaps Pharmscitech* 2016, 17, 20–42, doi: 10.1208/s12249-015-0360-7.
17. Tambe, S.; Jain, D.; Agarwal, Y.; Amin, P. Hot-Melt Extrusion: Highlighting Recent Advances in Pharmaceutical Applications. *Journal of Drug Delivery Science and Technology* 2021, 63, 102452, doi:10.1016/j.jddst.2021.102452.
18. Fan, R.; Chuan, D.; Hou, H.; Chen, H.; Xu, J.; Guo, G. Development and Evaluation of a Novel Biodegradable Implants with Excellent Inflammatory Response Suppression Effect by Hot-Melt Extrusion. *European Journal of Pharmaceutical Sciences* 2021, 166, 105981, doi:10.1016/j.ejps.2021.105981.
19. Munnangi, S.R.; Youssef, A.A.A.; Narala, N.; Lakkala, P.; Vemula, S.K.; Alluri, R.; Zhang, F.; Repka, M.A. Continuous Manufacturing of Solvent-Free Cyclodextrin Inclusion Complexes for Enhanced Drug Solubility via Hot-Melt Extrusion: A Quality by Design Approach. *Pharmaceutics* 2023, 15, 2203, doi:10.3390/pharmaceutics15092203.
20. Maniruzzaman, M.; Boateng, J.S.; Snowden, M.J.; Douroumis, D. A Review of Hot-Melt Extrusion: Process Technology to Pharmaceutical Products. *International Scholarly Research Notices* 2012, 2012, doi: 10.5402/2012/436763.
21. Darji, M.; Pradhan, A.; Vemula, S.K.; Kolter, K.; Langley, N.; Repka, M.A. Development of Delayed-Release Pellets of Ibuprofen Using Kollicoat® MAE 100P via Hot-Melt Extrusion Technology. *J Pharm Innov* 2023, doi:10.1007/s12247-023-09758.
22. Crowley, M.M.; Zhang, F.; Repka, M.A.; Thumma, S.; Upadhye, S.B.; Kumar Battu, S.; McGinity, J.W.; Martin, C. Pharmaceutical Applications of Hot-Melt Extrusion: Part I. Drug Development and Industrial Pharmacy 2007, 33, 909–926, doi:10.1080/03639040701498759.
23. Narala, S.; Nyavanandi, D.; Alzahrani, A.; Bandari, S.; Zhang, F.; Repka, M.A. Creation of Hydrochlorothiazide Pharmaceutical Cocrystals via Hot-Melt Extrusion for Enhanced Solubility and Permeability. *AAPS PharmSciTech* 2022, 23, 56, doi: 10.1208/s12249-021-02202-8.
24. Repka, M.A.; Gutta, K.; Prodduturi, S.; Munjal, M.; Stodghill, S.P. Characterization of Cellulosic Hot-Melt Extruded Films Containing Lidocaine. *European Journal of Pharmaceutics and Biopharmaceutics* 2005, 59, 189–196, doi: 10.1016/j.ejpb.2004.06.008.
25. Butreddy, A.; Sarabu, S.; Almutairi, M.; Ajjarapu, S.; Kolimi, P.; Bandari, S.; Repka, M.A. Hot-Melt Extruded Hydroxypropyl Methylcellulose Acetate Succinate Based Amorphous Solid Dispersions: Impact of Polymeric Combinations on Supersaturation Kinetics and Dissolution Performance. *International Journal of Pharmaceutics* 2022, 615, 121471, doi.org/10.1016/j.ijpharm.2022.121471.
26. Mididoddi, P.K.; Repka, M.A. Characterization of Hot-Melt Extruded Drug Delivery Systems for Onychomycosis. *European Journal of Pharmaceutics and Biopharmaceutics* 2007, 66, 95–105, doi: 10.1016/j.ejpb.2006.08.013.
27. Youssef, A.; Dudhipala, N.; Majumdar, S. Ciprofloxacin Loaded Nanostructured Lipid Carriers Incorporated into In-Situ Gels to Improve Management of Bacterial Endophthalmitis. *Pharmaceutics* 2020, 12, 572, https://doi.org/10.3390/pharmaceutics12060572.
28. Muhindo, D.; Ashour, E.A.; Almutairi, M.; Repka, M.A. Development and Evaluation of Raloxifene Hydrochloride-Loaded Subdermal Implants Using Hot-Melt Extrusion Technology. *International Journal of Pharmaceutics* 2022, 622, 121834, https://doi.org/10.1016/j.ijpharm.2022.121834.
29. Manimaran, V.; Damodharan, N. Development of Fast-Dissolving Tablets of Amlodipine Besylate by Solid Dispersion Technology Using Poloxamer 407 and Poloxamer 188. *Asian J Pharm Clin Res* 2017, 10, 135–141, https://doi.org/10.22159/ajpcr.2017.v10i7.17686.

30. Hadžidedić, Š.; Uzunović, A.; Šehić Jazić, S.; Kocova El-Arini, S. The Impact of Chirality on the Development of Robust and Stable Tablet Formulation of (S-) Amlodipine Besylate. *Pharmaceutical Development and Technology* 2014, 19, 930–941, doi:10.3109/10837450.2013.840847.
31. Silva, A.C.M.; Gállico, D.A.; Guerra, R.B.; Perpétuo, G.L.; Legendre, A.O.; Rinaldo, D.; Bannach, G. Thermal Stability and Thermal Decomposition of the Antihypertensive Drug Amlodipine Besylate. *J Therm Anal Calorim* 2015, 120, 889–892, doi:10.1007/s10973-014-3992.
32. Kelly, C.A.; Harrison, K.L.; Leeke, G.A.; Jenkins, M.J. Detection of Melting Point Depression and Crystallization of Polycaprolactone (PCL) in ScCO<sub>2</sub> by Infrared Spectroscopy. *Polymer journal* 2013, 45, 188–192, doi:10.1038/pj.2012.113.
33. Jana, S.; Leung, M.; Chang, J.; Zhang, M. Effect of Nano-and Micro-Scale Topological Features on Alignment of Muscle Cells and Commitment of Myogenic Differentiation. *Biofabrication* 2014, 6, 035012, doi: 10.1088/1758-5082/6/3/035012.
34. Dos Santos, T.M.B.K.; Merlini, C.; Aragones, Á.; Fredel, M.C. Manufacturing and Characterization of Plates for Fracture Fixation of Bone with Biocomposites of Poly (Lactic Acid-Co-Glycolic Acid) (PLGA) with Calcium Phosphates Bioceramics. *Materials Science and Engineering: C* 2019, 103, 109728, <https://doi.org/10.1016/j.msec.2019.05.013>.
35. Rai, A.; Sharma, S. Preparation and Evaluation of Oral Dispersible Formulations of Amlodipine Besylate. *Asian Journal of Pharmaceutical Research and Development* 2019, 7, 43–56, doi:10.22270/ajpr.v7i5.560
36. Dahima, R.; Pachori, A.; Netam, S. Formulation and Evaluation of Mouth Dissolving Tablet Containing Amlodipine Besylate Solid Dispersion. *International Journal of ChemTech Research* 2010, 2, 706–715.
37. Gokalp, N.; Ulker, C.; Guvenilir, Y.A. Synthesis of Polycaprolactone via Ring Opening Polymerization Catalyzed by Candida Antarctica Lipase B Immobilized onto an Amorphous Silica Support. *J. Polym. Mater* 2016, 33, 87–100.
38. Elzein, T.; Nasser-Eddine, M.; Delaite, C.; Bistac, S.; Dumas, P. FTIR Study of Polycaprolactone Chain Organization at Interfaces. *Journal of colloid and interface science* 2004, 273, 381–387, <https://doi.org/10.1016/j.jcis.2004.02.001>.
39. Singh, G.; Kaur, T.; Kaur, R.; Kaur, A. Recent Biomedical Applications and Patents on Biodegradable Polymer-PLGA. *Int. J. Pharmacol. Pharm. Sci* 2014, 1, 30–42.
40. Erbetta, C.D.C.; Alves, R.J.; Magalh, J.; de Souza Freitas, R.F.; de Sousa, R.G. Synthesis and Characterization of Poly (D, L-Lactide-Co-Glycolide) Copolymer. 2012, doi:10.4236/jbnb.2012.32027.
41. Li, C.; Cheng, L.; Zhang, Y.; Guo, S.; Wu, W. Effects of Implant Diameter, Drug Loading and End-Capping on Praziquantel Release from PCL Implants. *International journal of pharmaceutics* 2010, 386, 23–29, doi: 10.1016/j.ijpharm.2009.10.046.
42. Kim, T.-H.; Yun, Y.-P.; Park, Y.-E.; Lee, S.-H.; Yong, W.; Kundu, J.; Jung, J.W.; Shim, J.-H.; Cho, D.-W.; Kim, S.E. In Vitro and in Vivo Evaluation of Bone Formation Using Solid Freeform Fabrication-Based Bone Morphogenic Protein-2 Releasing PCL/PLGA Scaffolds. *Biomedical Materials* 2014, 9, 025008, doi: 10.1088/1748-6041/9/2/025008.
43. He, P.; Xu, S.; Guo, Z.; Yuan, P.; Liu, Y.; Chen, Y.; Zhang, T.; Que, Y.; Hu, Y. Pharmacodynamics and Pharmacokinetics of PLGA-Based Doxorubicin-Loaded Implants for Tumor Therapy. *Drug Delivery* 2022, 29, 478–488, doi:10.1080/10717544.2022.2032878.
44. Stewart, S.A.; Domínguez-Robles, J.; Donnelly, R.F.; Larrañeta, E. Implantable Polymeric Drug Delivery Devices: Classification, Manufacture, Materials, and Clinical Applications. *Polymers* 2018, 10, 1379, doi: 10.3390/polym10121379.
45. Youssef, S.H.; Kim, S.; Khetan, R.; Afinjuomo, F.; Song, Y.; Garg, S. The Development of 5-Fluorouracil Biodegradable Implants: A Comparative Study of PCL/PLGA Blends. *Journal of Drug Delivery Science and Technology* 2023, 81, 104300, <https://doi.org/10.1016/j.jddst.2023.104300>.
46. Liu, G.; McEnnis, K. Glass Transition Temperature of Plga Particles and the Influence on Drug Delivery Applications. *Polymers* 2022, 14, 993, doi: 10.3390/polym14050993.

**Disclaimer/Publisher's Note:** The statements, opinions and data contained in all publications are solely those of the individual author(s) and contributor(s) and not of MDPI and/or the editor(s). MDPI and/or the editor(s) disclaim responsibility for any injury to people or property resulting from any ideas, methods, instructions or products referred to in the content.